Cerebral Cortex December 2008;18:2855–2867
doi:10.1093/cercor/bhn044
Advance Access publication April 9, 2008

Hearing Loss Alters the Subcellular Distribution of Presynaptic GAD and Postsynaptic $GABA_A$ Receptors in the Auditory Cortex

Emma C. Sarro[1], Vibhakar C. Kotak[1], Dan H. Sanes[1,2] and Chiye Aoki[1,2]

[1]Center for Neural Science and [2]Department of Biology, New York University, New York, NY 10003, USA

We have shown previously that auditory experience regulates the maturation of excitatory synapses in the auditory cortex (ACx). In this study, we used electron microscopic immunocytochemistry to determine whether the heightened excitability of the ACx following neonatal sensorineural hearing loss (SNHL) also involves pre- or postsynaptic alterations of GABAergic synapses. SNHL was induced in gerbils just prior to the onset of hearing (postnatal day 10). At P17, the gamma-aminobutyri acid type A ($GABA_A$) receptor's β2/3-subunit ($GABA_Aβ2/3$) clusters residing at plasma membranes in layers 2/3 of ACx was reduced significantly in size ($P < 0.05$) and number ($P < 0.005$), whereas the overall number of immunoreactive puncta (intracellular + plasmalemmal) remained unchanged. The reduction of $GABA_Aβ2/3$ was observed along perikaryal plasma membranes of excitatory neurons but not of GABAergic interneurons. This cell-specific change can contribute to the enhanced excitability of SNHL ACx. Presynaptically, GABAergic axon terminals were significantly larger but less numerous and contained 47% greater density of glutamic acid decarboxylase immunoreactivity ($P < 0.05$). This suggests that GABA synthesis may be upregulated by a retrograde signal arising from lowered levels of postsynaptic $GABA_AR$. Thus, both, the pre- and postsynaptic sides of inhibitory synapses that form upon pyramidal neurons of the ACx are regulated by neonatal auditory experience.

Keywords: β2/3 subunits, deafness, development, electron microscopy, immunocytochemistry

Introduction

Synapse function is regulated homeostatically by an ongoing level of network activity (Turrigiano 2007). In the auditory system, deafferentation leads to enhanced excitability of subcortical regions (Kitzes 1984; Kitzes and Semple 1985; McAlpine et al. 1997; Mossop et al. 2000; Salvi et al. 2000). Brain slice experiments in the auditory brainstem as well as in the auditory midbrain demonstrate that significantly weaker inhibitory transmission may contribute (Kotak and Sanes 1996; Vale et al. 2004). At the postsynaptic side, this has been correlated with dysfunction of the chloride cotransporter, KCC2 (Vale et al. 2003). In the inferior colliculus, gamma-aminobutyric acid (GABA) synthesis and release may also be regulated in an activity-dependent manner (Abbott et al. 1999; Milbrandt et al. 2000; Mossop et al. 2000).

Recently, we turned our attention to the auditory cortex (ACx), as this region is also reported to respond to peripheral organ damage (Rajan 1998). In layer 2/3 (L2/3) pyramidal cells of developing gerbil ACx, total sensorineural hearing loss (SNHL) raised cortical excitability, and this was associated with an increased immunoreactivity of N-methyl-D-asparate receptor's NR2B subunits at excitatory synapses (Kotak et al. 2005). This study also showed diminished intracortically evoked inhibitory potentials in the same region. However, the mechanisms and loci of change at inhibitory synapses of the ACx remain unknown. To address these questions, we examined functional markers at pre- and postsynaptic loci of inhibitory synapses in L2/3 of ACx following SNHL. Specifically, we examined the subcellular localization of the β2 and β3 subunits of the gamma-aminobutyric acid type A ($GABA_A$) receptor ($GABA_Aβ2/3$) in relation to inhibitory synapses. We chose to analyze these subunits because they are expressed most consistently in mammalian cortex and play an obligatory role in agonist binding (Wisden et al. 1992; Amin and Weiss 1993; McKernan and Whiting 1996; for review see, Möhler 2006). At the presynaptic locus, we evaluated the levels of glutamic acid decarboxylase (GAD), the rate-limiting enzymes in GABA synthesis.

Our study reveals that SNHL induces changes to both sides of GABAergic synapses: postsynaptically, $GABA_Aβ2/3$ are displaced from the plasma membrane, while presynaptically, the level of GAD is increased within the terminals. These results are in agreement with the electrophysiological evidence showing reductions in $GABA_Aβ2/3$ function and a greater release of GABA in ACx of SNHL animals (Kotak et al. forthcoming). The unexpected increase of presynaptic GAD may reflect a compensatory response either to the postsynaptic removal of $GABA_A$ receptors from the plasma membrane or a failure of proper trafficking to the plasma membrane.

Methods

The Rationale for SNHL

The auditory system is unlike other sensory systems in having bilateral convergence at subcortical levels. This property of the auditory pathway precluded comparisons of monaural versus binaural regions within the cerebral cortex and led us to make comparisons across bilaterally deprived and nondeprived animals.

Surgery for SNHL

All protocols were reviewed and approved by New York University Institutional Animal Care and Use Committee. Bilateral cochlear ablations were performed on gerbil (*Meriones unguiculatus*) pups at P10, just prior to the onset of response to airborne sound. Details were as described previously (Sanes et al. 1992; Vale and Sanes 2002). In brief, gerbil pups were anesthetized (methoxyflurane), and each cochlea was rapidly removed with forceps. Animals were reared for 7 days with their parents under conditions identical to those of control pups. The age of surgery was chosen based on evidence that anteroventral cochlear nucleus cell number is unaffected by cochlear ablation after P9 (Tierney et al. 1997). Cochlea removal was confirmed post mortem by opening each cochlea under a dissecting microscope and finding the absence of cochlear tissue but gelfoam in its place.

Tissue Preparation

Three normal and 3 SNHL animals were anesthetized at P17 with 5% chloral hydrate (i.p.) and perfused transcardially with 4% paraformaldehyde, buffered with 0.1 M phosphate buffer (PB) to pH 7.4. Glutaraldehyde was omitted from the perfusate so as to preserve antigenicity. Brains were removed from skull and postfixed in the same fixative until sectioning. On the day of sectioning, the brains were transferred to PB. Eighty-micrometer-thick horizontal sections were prepared from the left hemisphere using a vibratome (Leica Microsystems, Nussloch, Germany), with the lateral side elevated 15°. These angles were the settings used for the physiological experiments (Kotak et al. 2005, forthcoming) and have the advantage of preserving the thalamo-cortical tracts and, thus, allowing for electrophysiological verification of the thalamo-recipient zone of ACx. Sections containing the thalamo-cortical tracts appeared at about 2–3 mm from the ventral surface. These sections were stored free-floating in a buffer of PB (pH 7.4) with 0.9% sodium chloride and 0.05% sodium azide (PBS-azide) at 4°C until antibody incubation.

Source and Specificity of Primary Antibodies

The anti-$GABA_A\beta2/3$ was purchased from Chemicon (Temecular, CA; catalog no. MAB341, formerly Roche's 1381458). This is a monoclonal antibody from clone BD17. Specificity of this antibody has been characterized extensively by a number of groups. Specifically, the antibody immunoprecipitates the $GABA_A$/benzodiazepine receptor complex purified from homogenates of bovine cortex and rodent cerebellum (Häring et al. 1985) and exhibits immunoreactivity to HEK cells transfected with the $GABA_A\beta2/3$ subunits but not those transfected with α1–6, β1, γ1, γ2, δ, or gly 48k subunits (Ewert et al. 1990). Electron microscopic immunocytochemistry has shown that this antibody recognizes symmetric synapses formed by GABA-enriched axon terminals, as well as intracellular membranous organelles (Richards et al. 1987; Fujiyama et al. 2002; Charara et al. 2005). In our hands, light microscopy revealed that this antibody immunolabels puncta surrounding unlabeled perikarya in L2/3 of gerbil ACx, (Fig. 1*A,B*) which, by electron microscopy, were identifiable as immunoreactivity associated with symmetric synapses (detailed under section Results). These patterns agree well with previous reports of light and electron microscopic immunocytochemistry.

The antibody directed against GAD 65/67 was purchased from Chemicon (catalog no. AB1511). This antibody has also been characterized extensively. Specifically, this antibody recognizes the 2 protein bands of expected molecular weights (65 and 67 kDa) in Western blots and immunoprecipitates GAD. Within intact tissue, the antibody immunolabels axon terminals forming symmetric synapses and approximately 5% of the neuronal perikarya residing in the cerebral cortex (Mugnaini and Oertel 1985; Muzio et al. 2002; Meier and Grantyn 2004; Tongjaroenbungam et al. 2004). These immunolabeling patterns agree well with our observations by light microscopy (Fig. 1*C,D*) and electron microscopy (detailed under section Results).

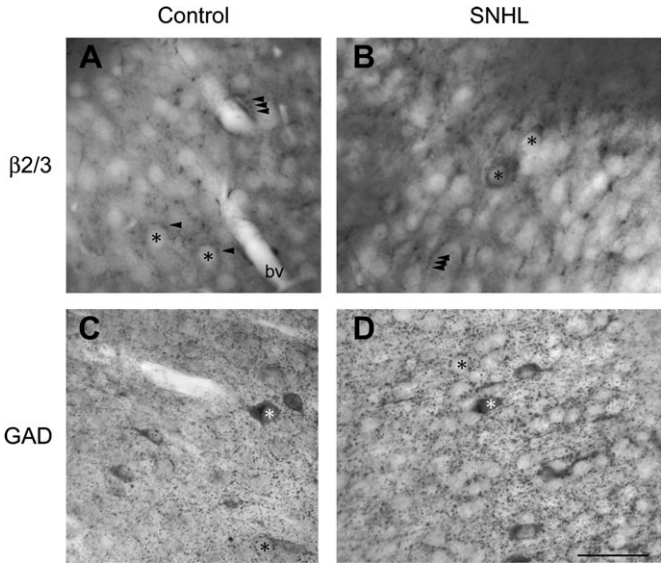

Figure 1. Light microscopic localization of $GABA_A\beta2/3$ subunits and GAD in the ACx. (*A* and *B*) The antibody directed against the $GABA_A\beta2/3$ subunits recognizes puncta (arrowheads) surrounding unlabeled cell bodies in layers 2/3 of Control ACx (asterisks in the nucleoplasm, *A*). The same antibody labels the perikaryal cytoplasm of a few neurons in an age-matched, SNHL ACx (asterisks in the nucleoplasm, *B*). Some of the puncta appear strung together (triple arrowheads in *A* and *B*). bv = blood vessel lumen. (*C* and *D*) The antibody directed against GAD65/67 recognizes puncta that surround unlabeled perikarya (black asterisks) of control (*C*) and SNHL (*D*) animals. In addition, some of the neuronal perikarya are intensely immunoreactive (white asterisks). Calibration bar = 50 μm for all panels.

Immunocytochemical Procedure

Both 3,3′-diaminobenzidine HCl (DAB) and silver-intensified colloidal gold (SIG) immunolabeling techniques were employed to mark the antigenic sites (Aoki et al. 2000). The DAB label was used to optimize detection of antigens, whereas SIG label was used to quantify the plasmalemmal versus intracellular sites of immunoreactivity. Sections derived from 3 SNHLs and 3 control animals were incubated and rinsed strictly in parallel and with no more than 10-s differences among the 6 sets of sections, so as to minimize interanimal variabilities arising from immunocytochemical (ICC) procedure.

Four to 6 left-hemisphere sections containing ACx from each of the 6 animals were incubated for 30 min in PBS-azide containing 1% bovine serum albumin (Sigma Chemicals, St Louis, MO) (PBS–bovine serum albumin [BSA]–azide, pH 7.4) to block any nonspecific immunolabeling. These sections were then incubated on a shaker for 3 days at room temperature in PBS–BSA–azide containing 1 of 2 primary antibodies, mouse anti-$GABA_A\beta2/3$ (1:50) or rabbit anti-GAD65/67 (1:400). This and all subsequent incubation steps were followed by 3 rinses in PBS (pH 7.4).

For immunolabeling with DAB, sections were incubated in biotinylated goat anti-mouse IgG, following the anti-$GABA_A\beta2/3$-subunit antibody incubation or in goat anti-rabbit IgG, following the anti-GAD antibody incubation (Vector Laboratories, Burlingame, CA), both at dilutions of 1:100 (15 μg/ml) for 1 h at room temperature. Sections were then incubated in the ABC solution (Elite Kit, Vector Laboratories, Burlingame, CA) for 30 min and immersed in PBS (pH 7.4) containing 0.3% DAB with 0.03% hydrogen peroxide (H_2O_2) as its substrate. Reaction time was 6 min ± 5 s for all sections. The peroxidase reaction was terminated by immersing sections in PBS. This ICC reaction was followed by multiple postfixation steps to preserve ultrastructure: 1% glutaraldehyde with PBS (pH 7.4) for 10 min; 1% osmium tetroxide (in 0.1 M PB) for 1 h; and 1% uranyl acetate in 70% ethanol, overnight.

For $GABA_A\beta2/3$ immunolabeling with SIG, sections were incubated for 4 h in ultrasmall (0.8 nm) gold-conjugated goat anti-mouse IgG (Electron Microscopy Sciences, Washington, PA) at a dilution of 1:100 in PBS–BSA (pH 7.6). For GAD65/67 immunolabeling with SIG, sections were incubated identically, except that the secondary antibody was 0.8-nm gold-conjugated anti-rabbit IgG (Electron Microscopy Sciences, Washington, PA). Sections were then postfixed in 1% glutaraldehyde with PBS (pH 7.4) for 10 min to cross-link antibodies to antigenic sites prior to silver intensification. To prepare sections for silver intensification, sections were rinsed for 1 min in 0.2 M citrate buffer (pH 7.4). These sections were immersed into the silver intensification reagent (Silver IntensEM Kit, Amersham, Buckinghamshire, UK) at room temperature for 12 min. The duration of the silver intensification step differed by no more than 10 s among the samples. Silver intensification was terminated by rinsing sections in citrate buffer. These sections were stored in PBS overnight. On the following day, sections underwent osmium-free processing (Aoki et al. 2000) to preserve membranes and ultrastructure as well as to prevent loss of the silver intensification by strong oxidants, such as osmium tetroxide. Analysis of the sizes of the SIG particles generated from GAD ICC revealed nearly identical distribution across tissue of the control and SNHL animals (mean values of the diameter: 59 ± 11 nm for Control tissue; 60 ± 12 nm for the SNHL tissue), indicating that the interanimal variability introduced during the silver intensification step was negligible. The

subsequent steps for embedding tissue in plastic were as described previously (Aoki et al. 2000; Aoki et al. 2007).

Controls were run to test the ability of both primary antibodies to recognize $GABA_A\beta2/3$ and GAD in gerbil. These sections were processed through identical steps in parallel with the experimental sections, with the exception that the 1st incubation did not contain primary antibodies. Immunolabeling was absent in these control sections.

Regions Analyzed for Data Collection

Ultrathin sections mounted on grids contained the thalamo-recipient region of the ACx. Areas of analysis focused on L2/3, lying just below layer 1. Layer 1 was identified by the smooth glia-lined pia mater dorsally and the lack of pyramidal neurons' somata (Kotak et al. 2005). We analyzed the surface-most portions of tissue, identified as the interface between the neuropil and plastic embedding material, where exposure to immunoreagents would be maximal.

All images were digitally captured using a CCD camera (AMT, MA) at a magnification of 30,000×. At this magnification, the neuropil area covered by each micrograph was approximately 19 μm^2. From each animal's ACx, approximately 20 micrographs (ca 380 μm^2) were captured for ultrastructural analyses. The software, ImageJ, Bethesda, MD (1.36b NIH), was used to measure areas within the captured images that were outside of the synaptic neuropil (i.e., areas occupied by the nucleoplasm, blood vessels or embedding matrix, only). The "Total Neuropil Area" reported in Tables 1 and 2 reflect this corrected value of synaptic neuropil area.

Identification of Ultrastructural Features

Because the analyses focused on changes at inhibitory synapses, it was necessary to differentiate symmetric (inhibitory) synapses from asymmetric (excitatory) synapses. A profile was identified to be axonic, based on the presence of multiple, small clear vesicles in the cytoplasm. The portion of the axon was identified to be synaptic where the axonal plasma membrane coursed parallel to the plasma membrane of another profile that was neither astrocytic nor axonal. The postsynaptic side was identified to be excitatory and asymmetric, if it was associated with an electron dense, postsynaptic density (PSD). Synapses without observable PSDs were identified as inhibitory.

Categorization of $GABA_A\beta2/3$ Labeling in ACx of SNHL and Control Animals' Tissues

Quantitative electron microscopy analysis was performed to determine whether neonatal SNHL affected the subcellular localization of the $GABA_A\beta2/3$-subunit labeling. Comparisons were made across the following 2 sensory rearing conditions: SNHL for 7 days versus intact (control), both at P17. Both DAB and SIG labels were used to characterize the subcellular localizations. Experimenters were blind to the sensory rearing conditions.

$GABA_A\beta2/3$ immunoreactivity occurring across 2 broad categories—intracellular versus plasmalemmal—were tallied. The intracellular sites were categorized further into 3 groups: axonal, dendritic, or somatic. The plasmalemmal sites were also categorized further as presynaptic, postsynaptic, or extrasynaptic. The label was identified as extrasynaptic if it occurred on the plasma membrane, but in a portion not abutting axon terminals or was removed from the parallel alignment of the pre- and postsynaptic membranes by more than 100 nm. Within both the SNHL and control tissues, the size of SIG particle clusters varied widely (Fig. 1*C*). However, as was stated above, the mean size of SIG clusters was nearly identical across sensory rearing conditions. SIG clusters were most commonly 60 nm in diameter. Thus, SIG particle clusters that occurred within 60 nm from the plasma membrane were categorized as plasmalemmal.

Quantification of $GABA_A\beta2/3$ Labeling in ACx of SNHL and Control Animals' Tissues

For each of the above 6 mutually exclusive subcellular categories, software of Adobe Photoshop (version 6.0; San Jose, CA) together with ImageJ (1.36b NIH), were used to calculate the area occupied by clusters of SIG particle aggregates. We also tallied the number of SIG clusters occurring within the 6 subcellular domains. Finally, the number of resolvable particles within a cluster was estimated by delineating the bumps that formed the outer contour of the clusters. These 3 methods of counting were done to avoid subjectivity in discerning the level of SIG immunolabeling. We accepted SIG particles of all sizes in our quantification. Each of the 3 procedures for SIG quantification underwent normalization by dividing the values of SIG level (particle number, SIG cluster number or SIG area) by the total SIG level encountered per animal. Consequently, the values shown in Tables 1 and 2 are expressed in units of "percent."

In contrast to the SIG particles, the DAB label was more diffuse. For the rare occasions when immunolabeling of DAB occurred continuously between both plasmalemmal and intracellular sites, a count of 1 was added to both categories. For each animal, we determined the proportion of total label occurring within each of the 6 subcellular regions introduced above. The tallies were also made to compare the relative distribution of immunolabel found intracellularly versus those on the plasma membranes.

Table 1

The subcellular localization of $GABA_A\beta2/3$, expressed as a percent of total immunoreactivity

Group	Total neuropil (μm^2)	Intracellular			Plasmalemmal		
		Axon	Dendrite	Soma	Presynaptic	Postsynaptic: dendrite/soma	Nonsynaptic or undetermined
A. β2/3 Immunolabeling by DAB							
SNHL	1032.06	13.24 ± 1.97	32.1 ± 1.15	8.81 ± 0.70	9.50 ± 1.81	8.62 ± 0.97	27.72 ± 1.03
Control	1050.49	8.11 ± 0.52	22.21 ± 1.7	3.36 ± 0.38	9.77 ± 1.44	15.33 ± 1.13	41.21 ± 2.22
P-value		$P > 0.1$	$P < 0.009$*	$P < 0.007$*	$P > 0.9$	$P < 0.02$*	$P < 0.02$*
B. β2/3 Immunolabeling by SIG: particle count							
SNHL	1062.64	11.4 ± 1.88	51.04 ± 1.38	7.1 ± 1.93	4.32 ± 1.58	22.46 ± 2.46	3.63 ± 0.21
Control	1039.13	6.57 ± 2.2	27.32 ± 5.22	3.31 ± 0.23	2.41 ± 1.23	59.20 ± 2.35	1.35 ± 0.4
P-value		$P > 0.1$	$P < 0.02$*	$P > 0.08$	$P > 0.3$	$P < 0.0005$*	$P < 0.008$*
C. β2/3 Immunolabeling by SIG: cluster count							
SNHL	1062.64	12.06 ± 1.66	38.0 ± 7.37	19.73 ± 10.8	7.72 ± 3.06	11.51 ± 1.55	10.98 ± 1.68
Control	1039.13	7.50 ± 2.64	21.61 ± 2.8	9.53 ± 0.72	8.93 ± 0.25	28.53 ± 1.97	23.88 ± 0.13
P-value		$P > 0.2$	$P > 0.1$	$P > 0.4$	$P > 0.7$	$P < 0.003$*	$P < 0.003$*
D. β2/3 Immunolabeling by SIG: cluster area							
SNHL	1062.64	9.18 ± 0.57	44.63 ± 2.14	9.47 ± 1.17	5.23±1.1	21.77 ± 2.16	9.79 ± 1.90
Control	1039.13	5.54 ± 1.43	29.06 ± 5.39	4.74 ± 0.94	1.58 ± 1.34	57.33 ± 2.83	1.66 ± 0.14
P-value		$P > 0.07$	$P > 0.05$	$P < 0.05$*	$P > 0.1$	$P < 0.0006$*	$P < 0.02$*

Note: Shown are mutually exclusive subcellular categories from the group means (±SEM) and *P*-values after immunolabeling by DAB (A), SIG particle count (B), SIG particle cluster count, and SIG area measurement (D). The "Total Neuropil" values reflect the total synaptic neuropil area that was surveyed. The areas occupied by blood vessels, the nucleoplasm, and the plastic embedding media facing the vibratome section surfaces were not included in these values.

Table 2
Measurements of axon terminals immunolabeled for GAD65/67 for each sensory condition

Group	Total neuropil (μm^2)	# Synaptic terminals	# Synaptic terminals/μm^2	Terminal area (μm^2)	Density (# SIG particles/μm^2)	Density (# SIG clusters/μm^2)	Density (SIG area/terminal area in %)
SNHL	1009.9	86	0.09 ± 0.002	0.44 ± 0.06	99.94 ± 4.02	24.53 ± 1.78	8.72 ± 0.10
Control	1105.4	123	0.10 ± 0.01	0.36 ± 0.02	67.79 ± 10.60	18.46 ± 1.35	5.83 ± 0.78
P-value			$P < 0.001$*	$P < 0.05$*	$P < 0.05$*	$P < 0.008$*	$P < 0.003$*

Note: Shown are the total amount of neuropil assessed for each group, the total number of axon terminals encountered in this analysis, the mean (±SEM) density of synaptic terminals, as well as the mean value of the area (±SEM) occupied by each axon terminal. Mean (±SEM) density of SIG immunolabeling/group are shown, using particles, particle clusters, and SIG area as units of counting.

Using these procedures, the SIG particle counts were higher than the counts obtained by DAB labeling. This difference arose from the discrete nature of SIG labels, which allowed us to count the number of particles contained within each cluster. In contrast, DAB labels were diffuse, leading us to count immunoreactivity that occurred as electron dense patches along the plasma membrane and as intracellular clumps.

For comparisons across the sensory conditions, we performed 2-tailed Student's *t*-test, assuming unequal variances. The significance level was set at $P < 0.05$.

Quantification and Comparison of GAD Labeling across SNHL and Intact Acx

GAD occurred in axons, dendrites and somata. Because we were interested in comparing presynaptic levels of GAD, only the presynaptic terminal profiles were included in the quantitative analysis. Presynaptic terminals were identified by the presence of more than a few vesicles in the cytoplasm. DAB immunolabeling was used mainly to assess the specificity of the antibody prior to quantifying GAD levels by SIG. Comparisons across sensory rearing conditions were performed for the following parameters: the number of GAD-immunoreactive terminals encountered per synaptic neuropil area surveyed; mean and SEM of the areas of presynaptic terminals encountered; GAD immunoreactivity within presynaptic terminals. These analyses of GAD axon terminals were performed upon 2-D images rather than 3-D reconstructions, because the immunolabeling is restricted to only the surface-most portions of vibratome sections. ImageJ (1.36b NIH) and a mouse pad (Wacom, Pearl model) were used to measure the area of presynaptic cytoplasmic profiles. GAD immunoreactivity within an axon terminal profile was quantified 3 ways, as was described for $GABA_A\beta2/3$ labeling: by counting the number of SIG particles within the axon terminal, counting the number of SIG particle clusters, and by using Image J to measure the area occupied by SIG clusters within the axon terminal. Each of these values was normalized to the area of the axon terminal. Comparisons across sensory conditions used the nonparametric statistical tests Mann–Whitney *U* as well as the Kolmogorov–Smirnov, with significance levels set at $P < 0.05$. The software, Statistica 6.1 (StatSoft, Tulsa, OK, 1984–2003), was used to perform the above-mentioned statistical tests. Experimenters were not blind to the conditions.

Results

The Subcellular Distribution of $GABA_A\beta2/3$ Immunolabeling

Both DAB and SIG labels were used as immunolabels to characterize the subcellular distributions of $GABA_A\beta2/3$ subunits. DAB-labeled β2/3 clusters were identified as electron dense aggregates that were at least 200% above the optical density of the plasma membrane as well as >2× the thickness of the plasma membrane (Fig. 2*A–D*). SIG-immunoreactivities were characterized as aggregates of maximally electron dense particles that formed larger particle clusters (Fig. 2*E–H*). The specificity of the $GABA_A\beta2/3$ antibody was confirmed by the absence of label in sections incubated without the primary antibody (Fig. 2*D,H*). Further, the absence of immunolabel at synapses with thick PSDs verified that the antibody did not cross-react with antigens of excitatory synapses. Label was also absent along the tissue–embed812 surfaces (Fig. 2*E,H*).

We 1st confirmed that, for both control and SNHL tissue, the $GABA_A\beta2/3$ immunolabel appeared along the postsynaptic membrane of symmetric synapses, as was shown previously in the brainstem of gerbils (Korada and Schwartz 1999) and elsewhere within the brain of other mammals (Richards et al. 1987; Fujiyama et al. 2002; Charara et al. 2005). Symmetric synapses were characterized by their lack of postsynaptic densities (PSD) but clear parallel alignment of the pre- and postsynaptic membranes. These symmetric synapses were sometimes found with the immunolabels concentrated more laterally within the synaptic cleft (Fig. 2*A,E,G*). Because this antibody is directed against the extracellular domain of the subunit, we expected the immunoreactivity to occur along the extracellular surface of the plasma membrane as well as in the lumen of membranous intracellular organelles. As expected, DAB labeling occurred within the synaptic cleft or overlying intracellular membranous organelles (Fig. 2*A–C*). SIG labeling was often centered over the synaptic cleft and intracellularly, whereas the membranous organelles could not be detected, presumably because they were obscured by the SIG particles (Fig. 2*E–G*).

Within or across sensory conditions, comparisons of the frequency of encounter with $GABA_A\beta2/3$ immunoreactivity per unit area revealed no significant difference, whether using DAB counts, SIG particle counts, SIG cluster counts or SIG cluster area measurements (*t*-test, $P > 0.5$ for all comparisons).

We then compared the distribution of $GABA_A\beta2/3$ immunoreactivity across the intracellular versus plasma membrane compartments. This analysis revealed that the ACx of control animals had a significantly higher proportion of immunolabels on plasma membranes than did the ACx of SNHL animals (Fig. 2*I,J*). Specifically, control tissue had an average of 66 ± 2% of $GABA_A\beta2/3$–DAB immunolabels associated with plasma membranes, although SNHL tissues exhibited only 46 ± 2% of the immunolabeling at the plasma membrane ($P < 0.002$, *t*-test) (Fig. 2*I*). Similarly, analysis of SIG cluster count showed that controls had an average of 61 ± 5% of $GABA_A\beta2/3$ immunolabels associated with the plasma membrane, whereas the SNHL tissue exhibited only 29 ± 4% of SIG labels at the plasma membrane ($P < 0.005$, *t*-test) (Fig. 2*J*). Likewise, analysis of SIG cluster areas revealed that 60.57 ± 4% of $GABA_A\beta2/3$ immunolabels are associated with plasma membranes of control tissue, whereas only 39.34 ± 3.5% occur at the plasmalemma of SNHL tissue ($P < 0.05$). The SNHL-to-Control differences were most prominent for labels occurring at the postsynaptic plasma membrane of dendrites and somata (Table 1).

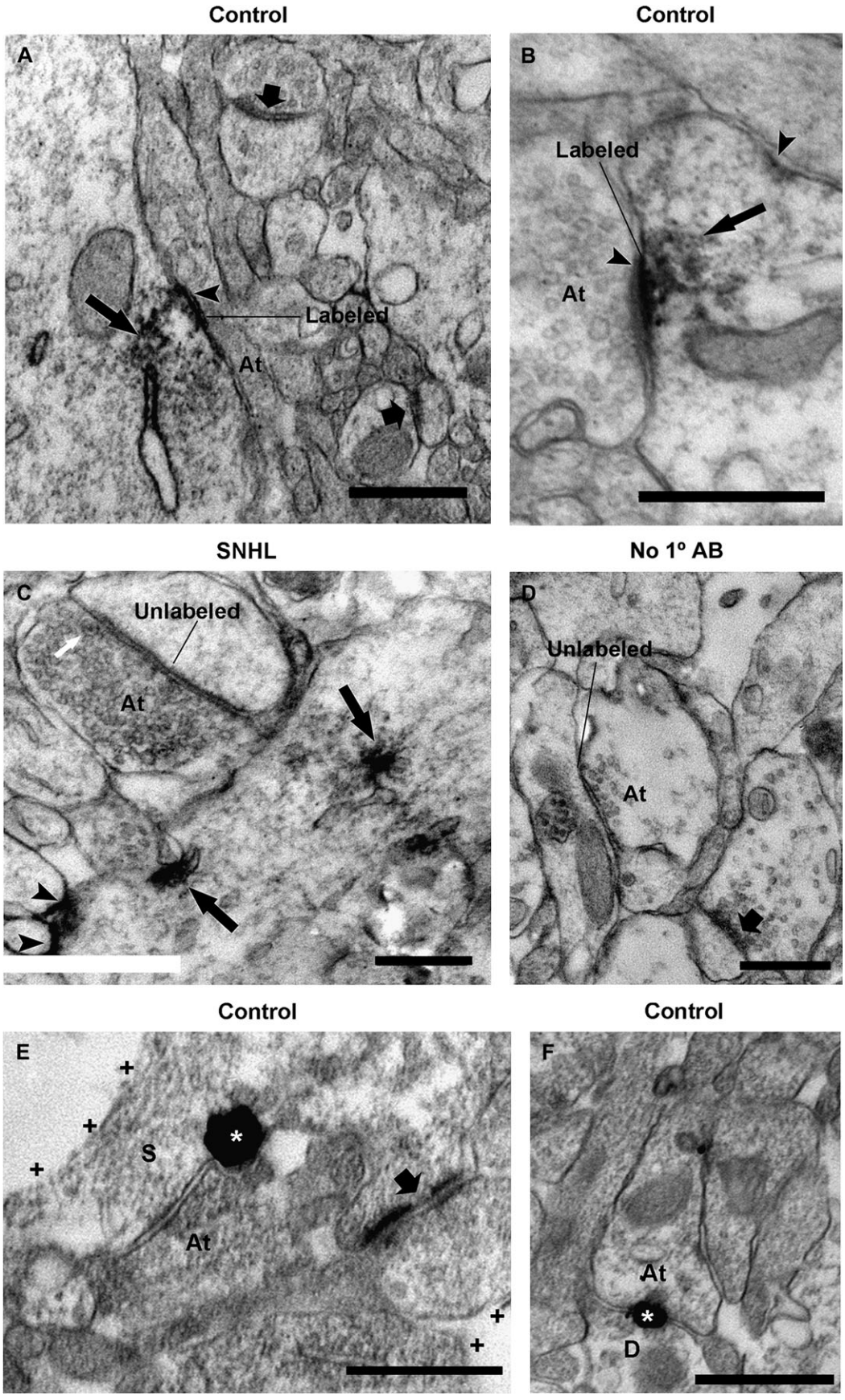

Figure 2.

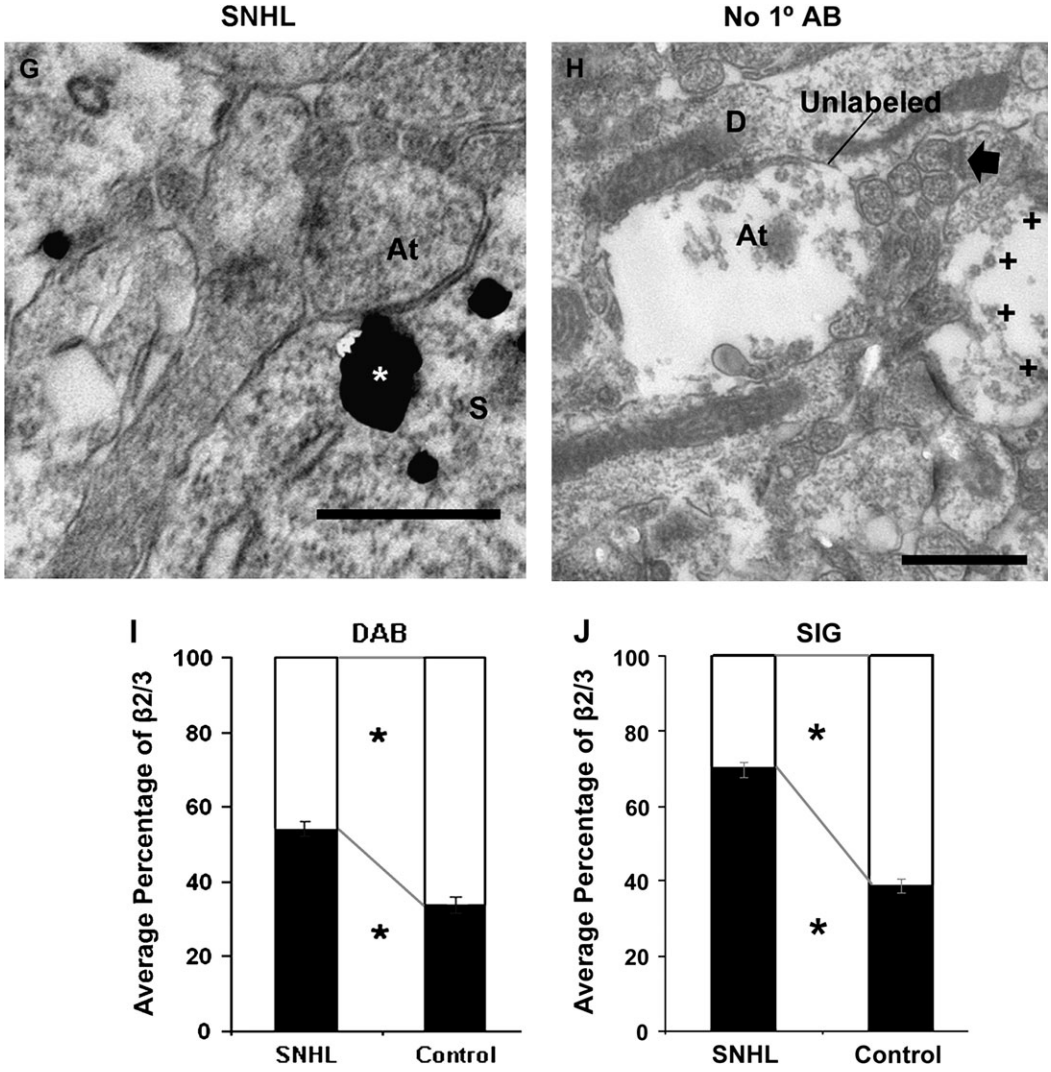

Figure 2. Electron micrographs showing examples of $GABA_A\beta2/3$ immunolabeling on the plasma membrane and at intracellular sites within layers 2/3 of ACx. $GABA_A\beta2/3$ immunolabeling is revealed by the DAB procedure in figures (*A*) to (*D*) and by the SIG procedure in figures (*E*) to (*H*). (*A*) Plasmalemmal labeling (arrowhead) at a perikaryon of a control animal's ACx. Immunoreactivity is at the symmetric synapse (arrowhead) and extends intracellularly (arrow) toward the endoplasmic reticulum. Such continuous labeling was tallied as labeled under both "intracellular" and "plasmalemmal" categories. Thick short arrows show lack of immunoreactivity at postsynaptic densities of asymmetric synapses. Here and in other panels, At = axon terminal. (*B*) Another example of plasmalemmal labeling, captured at a higher magnification. At this symmetric synapse (arrowhead), DAB labeling extends intracellularly (arrow). The same dendrite is juxtaposed to another axon (upper right), so identified by the presence of vesicles elsewhere. The dendritic plasma membrane facing this axon exhibits much less DAB labeling. (*C*) Patches of intracellular labeling (arrow) within a dendrite of an SNHL animal's ACx. The patches are near a clearly unlabeled symmetric (presumably inhibitory) synapse. This is further established by the presence of a dense-cored vesicle within the axon terminal (white arrow). Arrowheads point to plasmalemmal immunolabeling that are nonsynaptic. (*D*) A lack of DAB immunoreactivity in control sections incubated without the primary antibody at the site of a symmetric synapse and within the postsynaptic dendrite. (*E*) Cluster of SIG particles (white asterisk here and in *F* and *G*) at the junction between 2 plasma membranes forming a symmetric synapse onto a soma (S). A nearby asymmetric (presumably excitatory) synapse (arrow) is unlabeled. Note the tissue: Embed812 interface, marked by black crosses (+). Proximity of the sampled tissue to the tissue–Embed812 interface was intentional, to assure sampling from a region that was exposed maximally to immunoreagents. (*F*) Similar clustering of SIG particles at a symmetric synapse formed upon a dendrite (D). (*G*) SIG particles are found within the intracellular portion of a soma (S), near a symmetric synapse formed by the axon terminal, At. (*H*) Lack of SIG immunoreactivity at a symmetric synapse onto a distal dendrite as well within the intracellular portion of the dendrite in control tissue incubated without the primary antibody. (*I*) Quantitative analysis of $GABA_A\beta2/3$–DAB immunoreactivity encountered across the ACx from 3 controls and 3 SNHL animals. Cortices of control animals show a significantly higher proportion of total $GABA_A\beta2/3$ immunolabeling on plasma membranes (white bars). In contrast, cortices of SNHL animals show a significantly higher proportion of $GABA_A\beta2/3$ immunolabeling intracellularly (black bars), away from the plasma membranes. (*J*) Quantitative analysis of the SIG particle cluster distribution pattern. Cortices of control animals show a significantly higher proportion of total $GABA_A\beta2/3$ immunolabeling by SIG on plasma membranes (white bars), whereas cortices of SNHL animals show a significantly higher proportion of $GABA_A\beta2/3$ immunolabeling intracellularly (black bars), away from plasma membranes. Asterisks in (*I*) and (*J*) mark significance of $P < 0.002$, determined by 2-tailed Student's *t*-test. At, axon terminal; S, soma; D, dendrite. Scale bars = 500 nm.

GAD Immunoreactivity within Axon Terminals

We next sought to determine whether the hyperexcitability in ACx that follows SNHL (Kotak et al. 2005, forthcoming) might also occur through changes within presynaptic terminals of GABAergic synapses.

We 1st verified that GAD65/67 immunolabeling within the ACx of gerbils occur only within presynaptic terminals associated with symmetric synapses, indicating that this antibody does not cross-react with antigens of excitatory axon terminals (Fig. 3). Again, by using SIG as immunolabel, the GAD levels

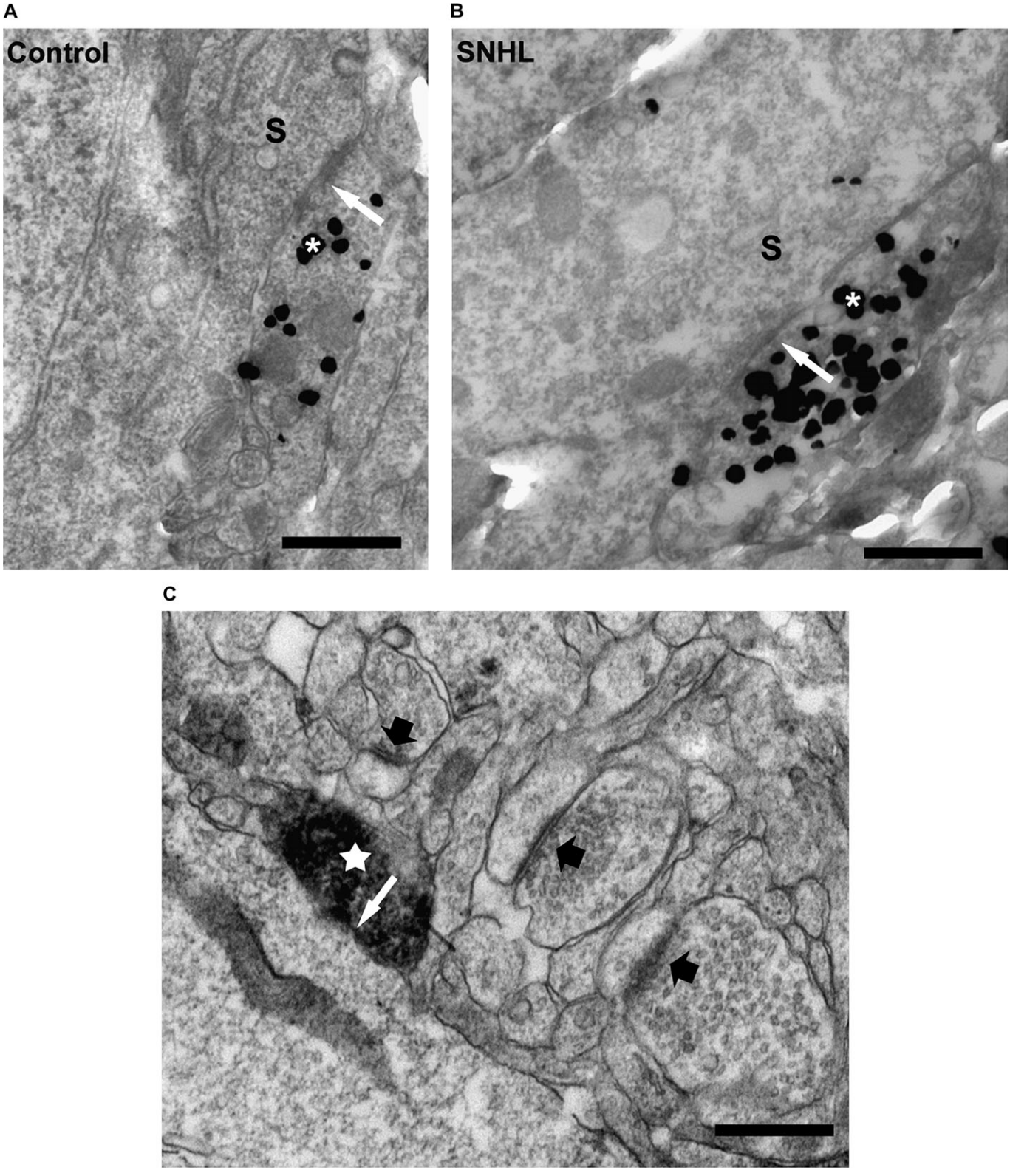

Figure 3. Electron micrographs show highly specific GAD65/67 immunolabeling of inhibitory axon terminals. (*A*, *B*) SIG immunolabeling (white asterisks) within inhibitory axon profiles forming symmetric (presumably inhibitory) synapses onto adjacent somata (S). White arrows denote active zones of the synapses. The density of SIG particles within the axon profiles is visibly lower in the tissue of the control (*A*) than of the SNHL (*B*) animal. (*C*) An axon terminal (white star) forming a symmetric synapse is intensely labeled with DAB. In contrast, the axon terminals forming asymmetric synapses (presumably excitatory, black arrows point to presynaptic membranes) are clearly unlabeled. Scale bars: 500 nm.

within the axon terminals were measured in 3 ways. The density of SIG particles and clusters per cytoplasmic area of axon terminals appeared to be higher in terminals from the SNHL animals than of the control animals (e.g., Fig. 3*A,B*). Indeed, analysis of over 200 axon terminals in the ACx revealed that the SNHL tissue had greater levels of GAD immunoreactivity, whether using SIG particle counts, SIG cluster counts or SIG area counts to quantify GAD levels (Fig. 4*A*, Table 2). Moreover, labeled axon terminals showing high levels of GAD (>100 SIG particles/μm^2) were more numerous in the ACx of SNHL animals (20% of axon terminals in brains of SNHL animals, compared with 7% in brains of control animals, Fig. 4*B*). In spite of these differences in the *number* of SIG particles and clusters, the distribution of SIG clusters according to size was remarkably similar across the 2 sensory conditions (Fig. 5, lower), indicating that the efficiency of the silver intensification procedure was adequately controlled across the tissue sets.

Unlike the levels of GAD within axon terminals, the mean value of the number of GAD-immunoreactive axon terminals encountered per unit area of synaptic neuropil was significantly higher in the ACx of controls (Table 2). The rate of encounter with a particular profile is dependent on the size of that profile (Mouton 2002). Therefore, we wondered whether the greater number of terminals encountered in the control group resulted from this group having larger axon profiles. This was not the case. On the contrary, the areas occupied by axon terminal profiles within 2-D images were larger for the ACx of SNHL animals than of controls (Table 2). This indicated that the difference we detected in the frequency of encounter with GAD terminals could not be due to size-differences.

Synaptic Levels of GABA$_A$β2/3

Analysis of the subcellular distribution of GABA$_A$β2/3 immunolabeling revealed that the frequency of immunoreactive patches along plasma membranes of SNHL ACx animals was most significantly reduced at postsynaptic sites within dendrites and somata (Table 1). For each of the 6 samples (3 SNHL and 3 controls), we also measured the total area occupied by SIG clusters at the postsynaptic membrane. Comparisons of this

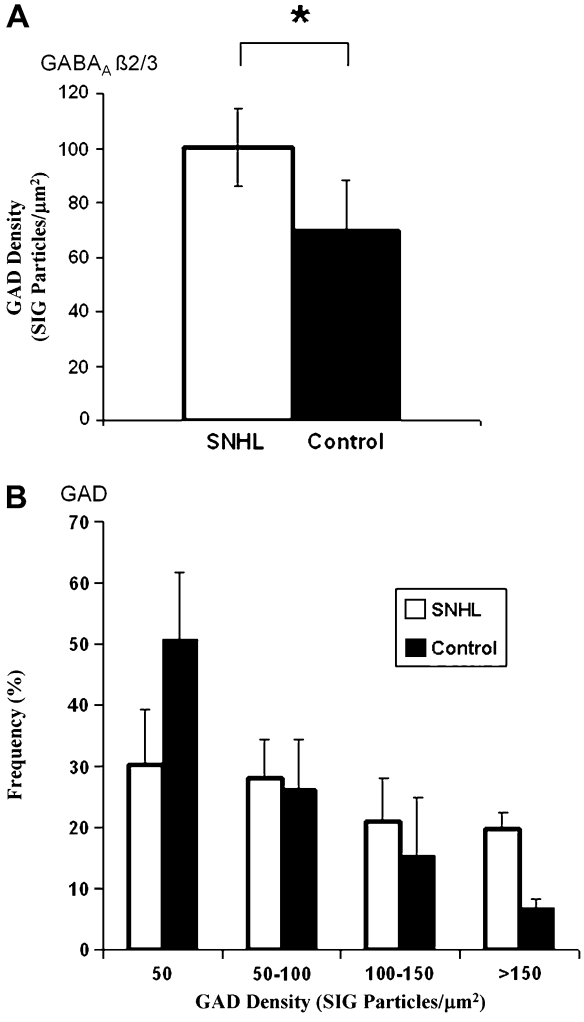

Figure 4. (*A*) The mean density of GAD within GABAergic inhibitory axon terminals. This value is significantly higher in cortices of SNHL animals than of controls. The values represent the group means for the density of GAD65/67–SIG particle counts within presynaptic terminals. The asterisk represents $P < 0.005$, determined by Kolmogorov–Smirnov test of independent groups. (*B*) Histogram compares the distribution of GAD density within axon profiles between both groups. There are proportionally more axon profiles which show higher GAD density levels (in SNHL animals>150 SIG particles/μm^2) than in control animals.

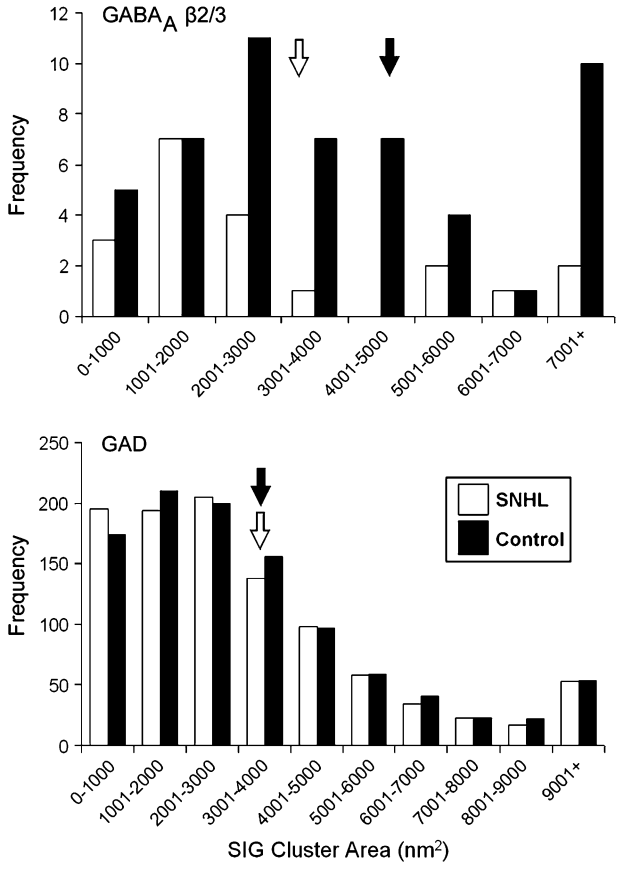

Figure 5. Comparison of the GABA$_A$β2/3 and GAD SIG cluster sizes across sensory rearing conditions. The upper graph shows the size distribution of the area of GABA$_A$β2/3 SIG clusters occurring along the postsynaptic plasma membrane of dendrites within ACx of Control and SNHL animals. The lower graph shows the size distribution of the area of GAD SIG clusters occurring within axon terminals of Control and SNHL animals Each SIG cluster was measured using Adobe Photoshop (version 6.0) and converted from pixels to the unit of nm^2. Arrows point to the mean values for each sensory rearing condition.

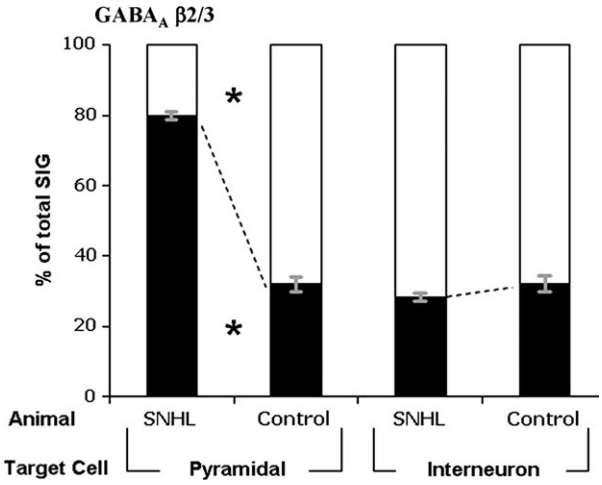

Figure 6. Somatic distribution of GABA$_A$ β2/3, as revealed by SIG labels. Somata of pyramidal neurons targeted by inhibitory axon terminals in cortices of SNHL animals show a significantly higher proportion of total β2/3 immunolabeling intracellularly (black bars) than in the ACx of control animals. Conversely, the ACx of controls have a significantly higher proportion of total GABA$_A$β2/3 immunolabeling on plasma membranes of pyramidal neurons (white bars). In contrast, the distribution of the GABA$_A$β2/3 immunolabeling within somata of interneurons do not show any significant difference between sensory rearing conditions. Asterisk marks significance ($P < 0.05$), determined by 2-tailed Student's *t*-test.

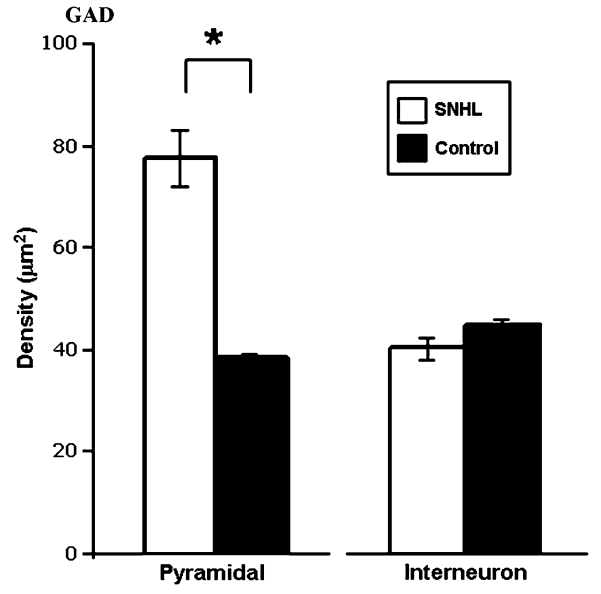

Figure 7. Density of GAD–SIG within axons targeting somata. The mean density of GAD particles within GABAergic axon terminals targeting somata of pyramidal neurons in the ACx of SNHL animals is significantly higher than the GAD levels targeting somata of pyramidal neurons in the control ACx. However, the mean density of GAD within GABAergic axon terminals targeting somata of interneurons is not significantly different between the 2 sensory rearing conditions. Asterisk marks significance of $P < 0.05$.

value revealed a significant difference across sensory rearing conditions (Table 1).

Dendritic Synapses

We extended this SIG analysis to determine whether SNHL affects the size as well as the frequency of individual GABA$_A$β2/3–SIG clusters at the postsynaptic plasma membrane of dendrites. The relative sizes of the SIG clusters reflecting GABA$_A$β2/3–SIG immunoreactivity at the dendritic plasma membrane was analyzed by using the software, ImageJ. This analysis revealed that SIG cluster size is also reduced significantly by SNHL ($P < 0.05$). Specifically, although the SIG cluster sizes of the SNHL and control ACx overlapped, the mean size of the SIG clusters were smaller for the SNHL ACx than of the control ACx (Fig. 5, upper) and rarely of the largest sizes found in the control ACx. It is unlikely that this difference in SIG cluster size distribution arose from differences in the ICC procedure, such as the duration of the silver intensification step, because the distribution of SIG cluster sizes of GAD was remarkably similar across the 2 sensory rearing conditions (Fig. 5, lower), even though the ICC procedure was identical for all. The reduced sizes of GABA$_A$β2/3–SIG clusters within the SNHL ACx may reflect reductions in the degree of the GABA$_A$β2/3 protein clustering along the plasma membrane of dendrites.

Axo-Somatic Synapses

The reduced expression of GABA$_A$β2/3 would lead to enhanced cortical excitability, but only if the postsynaptic neuron is excitatory. Although the identity of postsynaptic dendrites are difficult to identify by ultrastructural features, alone, the identity of somata is possible, because the nuclear envelopes are smooth for pyramidal neurons and invaginated for the inhibitory interneurons (Feldman 1984; Peters and Saint Marie 1984). We took advantage of this ultrastructural feature to distinguish the 2 potential types of neurons targeted axo-somatically by GABAergic axons. SIG-immunolabeled tissue from 2 SNHL and 2 control animals were used to analyze an average of 10 pyramidal cells and 5 interneurons per animal. This analysis revealed that 75 ± 1% of GABA$_A$β2/3–SIG particle counts is located intracellularly for the pyramidal cells of SNHL ACx. In contrast, the pyramidal cells of control ACx exhibit the GABA$_A$β2/3–SIG particle counts at intracellular sites at a rate of 29 ± 2% (Fig. 6). This difference was significant ($P < 0.05$, Student's *t*-test).

Although the pyramidal cells showed this sensory rearing-dependent differences in the subcellular distribution of GABA$_A$ β2/3–SIG immunolabeling, the inhibitory interneurons showed no difference in the subunit's subcellular distribution pattern across the 2 sensory conditions (Fig. 6, $P > 0.05$, Student's *t*-test).

GAD Levels at Axo-somatic Synapses

GAD level within GABAergic axon terminals also showed differences that were dependent upon sensory rearing condition and target cell-type: those axons that targeted somata of pyramidal neurons contained, on average, higher densities of GAD SIG particles within the ACx of SNHL animals than of control ACx ($P < 0.05$, Student's *t*-test, Fig. 7). In contrast, the axon terminals targeting inhibitory interneurons showed no difference in GAD across sensory rearing conditions (Fig. 7, $P > 0.05$).

Discussion

The major results of this study are that SNHL in developing gerbils leads to a reduction of GABA$_A$β2/3 localization at the postsynaptic plasma membrane and an increased density of GAD immunoreactivity within axon terminals of the ACx.

Furthermore, both the pre- and postsynaptic changes occur at synapses targeting excitatory pyramidal cells. Although the presence of $GABA_A$ receptors to the plasma membrane cannot, by itself, prove functionality of these receptors, displacement of the receptor subunits from the plasma membrane is a clear indication that these receptor subunits cannot be functional. Our finding is corroborated by electrophysiology—namely that SNHL ACx neurons display significantly smaller amplitudes of spontaneous and evoked $GABA_A$R–inhibitory postsynaptic currents and enhanced excitability (Kotak et al. 2005, forthcoming).

The increased level of presynaptic GAD is also corroborated by electrophysiology, in that this change could underlie the heightened probability of GABA release in the SNHL ACx (Kotak et al. forthcoming). The elevation of GAD at these synapses could reflect a homeostatic mechanism at the level of individual synapses, requiring a retrograde signal that links reduced postsynaptic efficacy to increased presynaptic efficacy (Petersen et al. 1997; Davis et al. 1998; Frank et al. 2006). In vitro manipulations have shown that the locus of change can be either pre- or postsynaptic, depending on the developmental stage (Wierenga et al. 2006). The present data, however, suggest that the locus of change in vivo is both pre- and postsynaptic.

Activity-Dependent Localization of $GABA_A\beta 2/3$ to the Postsynaptic Plasma Membrane

The majority of $GABA_A$ receptors are pentameric assemblies of subunits forming a Cl^--selective ion channel. $GABA_A$ receptor physiology is strongly determined by the subunit composition (Inglefield et al. 1994; MacDonald and Olsen 1994; McKernan and Whiting 1996; Browne et al. 2001). Both the β2 and β3 subunits are most abundantly expressed in mammalian cortex. These subunits play a role in agonist sensitivity by forming the binding sites for GABA and its potentiator, loreclezole (Wisden et al. 1992; Amin and Weiss 1993; Wafford et al. 1994; McKernan and Whiting 1996; Baumann et al. 2003; for review see, Möhler 2006). Thus, the reduction of postsynaptic β2/3 subunits agrees with recently collected physiology data, which is that loreclezole is ineffective in enhancing sIPSC duration in neurons of SNHL ACx (Kotak et al. forthcoming).

β Subunits are also essential for the localization of $GABA_A$ receptors to the synaptic membrane and for the formation of functional Cl^- anionophore (Connolly et al. 1996; Baumann et al. 2002). Accordingly, smaller-than-normal sIPSC amplitudes have previously been recorded in the reticular nucleus of β3-subunit knockout mice (Huntsman et al. 1994). In addition, the β-subunits provide a site for kinase-dependent phosphorylation (Browning et al. 1990). Therefore, the inadequate distribution of β subunits to the plasma membrane can alter agonist sensitivity and binding, as well as the post-translational regulation of $GABA_A$ receptors (Verdoorn et al. 1990; Ducic et al. 1995).

Structural evidence shows that a number of proteins exist to regulate the clustering and stabilization of $GABA_A$ receptors within the synaptic membrane (Caruncho et al. 1993; Jacob et al. 2005; Studler et al. 2005; for review, see Fritschy et al. 2003). The reduced sizes of $GABA_A\beta 2/3$ SIG clusters seen within the ACx of SNHL animals suggest that sizes of the $GABA_A$ receptor clusters may have been altered by this manipulation. Indeed, previous studies have shown that $GABA_A$ receptor trafficking is activity-dependent (Tehrani and Barnes 1991; Barnes 1996; Nusser et al. 1997, 1998). The reduced frequency and sizes of $GABA_A\beta 2/3$-immunoreactive patches at the postsynaptic plasma membrane following hearing loss could reflect faulty mobilization, insertion and/or cross-linking of $GABA_A$ receptors to lipid bilayers and submembrane anchors, because $GABA_A\beta 2/3$ counts were significantly higher intracellularly.

Stability of Presynaptic $GABA_A\beta 2/3$

In contrast to the changes observed for postsynaptic $GABA_A\beta 2/3$, the presynaptic expression of $GABA_A\beta 2/3$ was not significantly altered by SNHL. $GABA_A$ receptors expressed at axon terminals are reported to regulate the release of neurotransmitters other than GABA, such as glutamate (Turecek and Trussell 2002; Charara et al. 2005), by exerting presynaptic inhibition through axo-axonic junctions (Maxwell et al. 1990). Our findings point to the specificity in the response pattern of $GABA_A\beta 2/3$ to SNHL. The response is specific to GABAergic synapses formed on dendrites and somata, and not at axo-axonic junctions.

Comparisons with Earlier Findings Regarding $GABA_A$ Receptor Subunit Expression

Not all of the effects of SNHL we observe are congruent with other reports. At least some of the divergences could arise from methodological differences. For example, confocal microscopy has shown that bilateral cochlear ablation in adulthood leads to an increased expression of mRNA specific for $GABA_A$ receptor subunits β2, β3, and γ2 within cell bodies of the inferior colliculus as well as a rise of β3-subunit immunoreactivity there (Holt et al. 2005). Beyond the obvious difference of age, brain region and species, their use of confocal microscopy precluded assessment of changes specific to the postsynaptic plasma membrane. Conversely, although the elevated mRNA expression that they report would predict a rise of protein levels, our approach could not determine levels of the β2/3 protein.

Neonatal visual deprivation by dark rearing does not lead to a significant change in the total amount of [^{3}H] muscimol bound to receptors in cat visual cortex (Mower et al. 1986, 1988). A lack of difference in the total number of β2/3-immunoreactive sites—that is, the sum of cytoplasmic and plasmalemmal sites that we observe—is in agreement with the stability of muscimol binding sites in the visual cortex. However, although the procedure of [^{3}H] muscimol binding is useful for determining the molar concentration of GABA-binding sites within tissue, it does not differentiate ligand binding sites that occur specifically at the plasma membrane versus intracellularly, because both sites can participate in radioligand binding.

Besides differences arising from the histological techniques, differences may also arise from the form of deprivation employed. Fuchs and Salazar (1998) showed a decrease in [^{3}H] muscimol binding to $GABA_A$ receptors within the barrel cortex after whisker trimming during the 1st 6 postnatal weeks. The change was small (<10%) but significant, relative to the immediately adjacent, nondeprived columns. Perhaps our results will converge once we limit our sensory deprivation to a specific range of frequency.

Our quantification measures of SIG immunoreactivity on plasmalemmal sites as well as intracellular sites were strikingly consistent across the 3 modes of analysis. However, slight inconsistencies in the category of undetermined

immunoreactivity could have arisen from a less than optimal ultrastructural preservation for SIG than for DAB; that is, the omission of osmium tetroxide from the fixation protocol. This could have led to immunoreactive sites associated with unknown subcellular structures, including the surrounding glia (Bureau et al. 1995; Bekar et al. 1999). Despite this, it can be noted that the category of unidentifiable immunoreactivities was smaller than the sum of both other categories.

Presynaptic Plasticity of GAD Level

GAD level has been thought to reflect demand for GABA synthesis (Martin and Rimvall 1993; Rimvall and Martin 1994), such as during hippocampal hyperexcitability (Feldblum et al. 1990; Ramirez and Gutierrez 2001; Maqueda et al. 2003) and GABA release probability, as shown in the crayfish neuromuscular junction (Golan and Grossman 1996). Conversely, changes in excitability have been shown to also involve altered expression of vesicular and plasmalemmal GABA transporters (Hua et al. 2001; Hirao et al. 1998; Orozco-Suarez et al. 2000; Kang et al. 2003; Fueta et al. 2003; Bragina et al. 2007). We showed that the expression of GAD is not only activity-dependent but is also specific to the cell-type of the targeted cell. Perhaps our observed changes reflect an enhanced demand for GABA synthesis, due to heightened excitability of the glutamatergic/pyramidal cells and thus, of the ACx globally.

Although the response patterns of GAD to sensory deprivation may differ among isoforms and depend upon sensory modality and age, to our knowledge, none of the past studies assayed the levels of GAD specifically within axons. This may explain why our results of elevated levels of GAD differ from those reported in the auditory brainstem and other cortices following deafferentation. For example, GAD immunoreactivity declines in the neurons of IC after cochlear damage in adulthood (Milbrandt et al. 2000; Mossop et al. 2000), in V1 of deprived columns of adult monocular monkeys (Hendry and Jones 1988) and within deprived barrels of somatosensory cortex of mice after whisker trimming (Jiao et al. 2006). It is possible that this discrepancy is due to an augmented trafficking of GAD from the soma (measured by others) to axon terminals (measured by us) following sensory deprivation. Such coordinated changes across somata and axon terminals agree with works of Benson et al. (1989) and others (Bear et al. 1985; Silver and Stryker 2000; Mower and Guo 2001), who report no change in overall levels of GAD mRNA or immunoreactivity following sensory deprivation.

Morphological Changes to GAD Terminals

Our morphological analysis shows fewer but larger GAD positive terminal profiles in layers 2/3 of ACx of deafened animals. This suggests that activity during normal development may direct the larger precursor axon terminals to split into multiple, independent active zones. It is possible that the reduced number of terminals found in the SNHL ACx reflects retardation in the development of GABAergic axon terminals. Our findings agree with previous reports. Neonatal whisker trimming leads to fewer inhibitory synapses (Jiao et al. 2006) and GABAergic axon terminals (Micheva and Beaulieu 1995) in barrel cortex. Moreover, denervation of the cerebral cortex leads to an increase in bouton area at symmetric synapses in the upper layers of cerebral cortex (Rutledge 1978). Evidently, even if the morphological maturation of GABAergic axon terminals within SNHL brains is slower, they are still able to counter the heightened cortical excitability by upregulating GAD content in each terminal.

Comparisons with Other Models

In the visual and somatosensory systems, neonatal sensory deprivation causes robust alterations of intracortical connections (Trachtenberg and Stryker 2001) and receptive field properties (Shepherd et al. 2003). Cochlear removal before hearing onset is most analogous to enucleation and eyelid suture before eye opening. Neonatal monocular eyelid suture leads to increased spontaneous activity of layer 4 pyramidal neurons in the monocular zone of the deprived visual cortex hemisphere. This has been hypothesized to be due to a reduction in the inhibitory drive within layer 4 (Maffei et al. 2004). Our findings support this view.

The present findings are also consistent with reports of decreased GABAergic transmission in isolated cortical neurons. For example, in cultured visual cortical neurons, tetrodotoxin-induced activity blockade triggers a decline in the amplitude of miniature IPSC, the number of postsynaptic sites expressing the β subunit of $GABA_A$ receptors, and the number of open chloride channels (Kilman et al. 2002). In an adult model of age-related hearing loss, weakened inhibition is associated with changes in GABA receptor function, subunit composition, as well the levels of presynaptic GAD and GABA (Caspary et al. 1990, 1995, 1999). Thus, all of these studies, including ours, indicate that changes in GABA synapses involve concerted alterations across pre- and postsynaptic loci.

Future Directions

The differences we identified at pre- and postsynaptic sites of SNHL ACx may persist into adulthood and may also reflect immature features of GABAergic synapses that occur within the ACx prior to hearing onset. Future studies that examine the chemical and ultrastructural features of GABAergic synapses across multiple ages should be able to address these questions.

Supplementary Material

Supplementary material can be found at: http://www.cercor.odfordjournals.org/

Funding

National Institutes of Health DC006864 to D.H.S. and V.C.K.; and National Institutes of Health NS41091, EY13145, P30 EY13079, R01 DA00961809 and NYU Research Challenge Fund to C.A.

Notes

Conflict of Interest: None declared.

Address correspondence to Chiye Aoki, PhD. Center for Neural Science, New York University, 4 Washington Place, Rm. 809, New York, NY 10003, USA. Email: ca3@nyu.edu.

References

Abbott SD, Hughes LF, Bauer CA, Salvi R, Caspary DM. 1999. Detection of Glutamate Decarboxylase isoforms in rat inferior colliculus following acoustic exposure. Neuroscience. 93:1375–1381.

Amin J, Weiss DS. 1993. GABAA receptor needs two homologous domains of the beta-subunit for activation by GABA but not by pentobarbital. Nature. 366:565–569.

Aoki C, Mahodomrongkul V, Fujisawa S, Habersat R, Shirao T. 2007. Chemical and morphological alterations of spines within the

hippocampus and entorhinal cortex precedes the onset of Alzheimer's disease pathology in double knock-in mice. J Comp Neurol. 505:352–462.
Aoki C, Rodrigues S, Kurose H. 2000. Use of electron microscopy in the detection of adrenergic receptors. Methods Mol Biol. 126:535–63.
Barnes EM, Jr. 1996. Use-dependent regulation of GABAA receptors. Int Rev Neurobiol. 39:53–76.
Baumann SW, Baur R, Sigel E. 2002. Forced subunit assembly in α1β2γ2 GABAA receptors. J Biochem Chem. 277:46020–46025.
Baumann SW, Baur R, Sigel E. 2003. Individual properties of the two functional agonist sites in $GABA_A$ receptors. J Neurosci. 23:11158–11166.
Bear MF, Schmechel DE, Ebner FF. 1985. Glutamic acid decarboxylase in the striate cortex of normal and monocularly deprived kittens. J Neurosci. 5:1262–1276.
Bekar LK, Jabs R, Walz W. 1999. $GABA_A$ receptor agonists modulate K+ currents in adult hippocampal glial cells in situ. Glia. 26:129–138.
Benson DL, Isackson PJ, Hendry SH, Jones EG. 1989. Expression of glutamic acid decarboxylase mRNA in normal and monocularly deprived cat visual cortex. Brain Res Mol Brain Res. 5:279–287.
Bragina L, Melone M, Fattorini G, Conti F. 2007. Clozapine upregulates the expression of the vesicular GABA transporter (VGAT) in rat frontal cortex. Mol Psychol. 12:612–619.
Browne SH, Kang J, Akk G, Chiang LW, Schulman H, Huguenard JR, Prince DA. 2001. Kinetic and pharmacological properties of $GABA_A$ receptors in single thalamic neurons and GABAA subunit expression. J Neurophysiol. 86:2312–2322.
Browning MD, Bureau M, Dudek EM, Olsen RW. 1990. Protein kinase C and cAMP-dependent protein kinase phosphorylate the β subunit of the purified γ-aminobutyric acid A receptor. Proc Natl Acad Sci USA. 87:1315–1318.
Bureau M, Laschet J, Bureau-Heeren M, Hennuy B, Minet A, Wins P, Grisar T. 1995. Astroglial cells express large amounts of $GABA_A$ receptor protein in mature brain. J Neurochem. 65:2006–2015.
Caruncho HJ, Puia G, Slobodynasky E, Pinto Da Silva P, Costa E. 1993. Freeze-fracture immunocytochemical study of the expression of native and recombinant $GABA_A$ receptors. Brain Res. 603:234–242.
Caspary DM, Holder TM, Hughes LF, Milbrandt JC, McKernan RM, Naritoku DK. 1999. Age-related changes in $GABA_A$ receptor subunit composition and function in rat auditory system. Neuroscience. 93:307–312.
Caspary DM, Milbrandt JC, Helfert RH. 1995. Central auditory aging: GABA changes in the inferior colliculus. Exp Gerontol. 3–4:349–360.
Caspary DM, Raze A, Lawhorn Armour BA, Pippin J, Americ SP. 1990. Immunocytochemical and neurochemical evidence for age-related loss of GABA in the inferior colliculus: implications for neural presbycusis. J Neurosci. 10:2363–2372.
Charara A, Pare JF, Levey AI, Smith Y. 2005. Synaptic and extrasynaptic GABA-A and GABA-B receptors in the globus pallidus: an electron microscopic immunogold analysis in monkeys. Neuroscience. 131:917–933.
Connolly CN, Wooltorton JR, Smart TG, Moss SJ. 1996. Subcellular localization of gamma-aminobutyric acid type A receptors is determined by receptor beta subunits. Proc Natl Acad Sci USA. 93:9899–9904.
Davis GW, DiAntonio A, Petersen SA, Goodman CS. 1998. Postsynaptic PKA controls quantal size and reveals a retrograde signal that regulates presynaptic transmitter release in Drosophila. Neuron. 20:305–315.
Ducic I, Caruncho HJ, Zhu WJ, Vicini S, Costa E. 1995. γ-Aminobutyric acid gating of Cl- channels in recombinant GABAA receptors. J Pharmacol Exp Ther. 272:438–445.
Ewert M, Shivers BD, Lüddens H, Möhler H, Seeburg PH. 1990. Subunit selectivity and epitope characterization of mAbs directed against the $GABA_A$/benzodiazepine receptor. J Cell Biol. 110:2043–2048.
Feldblum S, Ackermann RF, Tobin AJ. 1990. Long-term increase of glutamate decarboxylase mRNA in a rat model of temporal lobe epilepsy. Neuron. 5:361–371.
Feldman ML. 1984. Morphology of the neocortical pyramidal neuron. In: Peters A, Jones EG, editors. Cerebral cortex, cellular components of the cerebral cortex. Vol. 1. New York: Plenum Press. p. 123–200.
Frank CA, Kennedy MJ, Goold CP, Marek KW, Davis GW. 2006. Mechanisms underlying the rapid induction and sustained expression of synaptic homeostasis. Neuron. 52:663–677.
Fritschy JM, Schweizer C, Brünig I, Lüscher B. 2003. Pre- and postsynaptic mechanisms regulating the clustering of type A γ-aminobutyric acid receptors ($GABA_A$ receptors). Biochem Soc Trans. 31:889–892.
Fuchs JL, Salazar E. 1998. Effects of whisker trimming on $GABA_A$ receptor binding in the barrel cortex of developing and adult rats. J Comp Neurol. 395:209–216.
Fueta Y, Vasilets LA, Takeda K, Kawamura M, Schwartz W. 2003. Down-regulation of GABA-transporter function by hippocampal translation product: its possible role in epilepsy. Neuroscience. 118:371–378.
Fujiyama F, Stephenson FA, Bolam JP. 2002. Synaptic localization of $GABA_A$ receptor subunits in the substantia nigra of the rat: effects of quinolinic acid lesions of the striatum. Eur J Neurosci. 15: 1961–1975.
Golan H, Grossman Y. 1996. Block of glutamate decarboxylase decreases GABAergic inhibition at the crayfish synapses: possible role of presynaptic metabotropic mechanisms. J Neurophysiol. 75:2089–2098.
Häring P, Stähli C, Schoch P, Takács B, Staehelin T, Möhler H. 1985. Monoclonal antibodies reveal structural homogeneity of γ-aminobutyric acid/benzodiazepine receptors in different brain areas. Proc Natl Acad Sci USA. 82:4837–4841.
Hendry SH, Jones EG. 1988. Activity-dependent regulation of GABA expression in the visual cortex of adult monkeys. Neuron. 1:701–712.
Hirao T, Morimoto K, Yamamoto Y, Watanabe T, Sato H, Sato K, Sato S, Yamada N, Tanaka K, Suwaki H. 1998. Time-dependent and regional expression of GABA transporter mRNAs following amygdala-kindled seizures in rats. Mol. Brain Res. 54:49–55.
Holt AG, Asako M, Lomax CA, MacDonald JW, Tong L, Lomax ML, Altschuler RA. 2005. Deafness-related plasticity in the inferior colliculus: gene expression profiling following removal of peripheral activity. J Neurochem. 93:1069–1086.
Hua YH, Hu JH, Zhao WJ, Fei J, Yu Y, Zhou XG, Mei ZT, Guo LH. 2001. Overexpression of γ-aminobutyric acid transporter subtype I leads to susceptibility to kainic acid-induced seizure in transgenic mice. Cell Res. 11:61–67.
Huntsman MM, Isackson PJ, Jones EG. 1994. Lamina-specific expression and activity-dependent regulation of seven GABA, receptor subunit mRNAs in monkey visual cortex. J Neurosci. 14:2236–2259.
Inglefield JF, Sieghart W, Kellogg CK. 1994. Immunohistochemical and neurochemical evidence for $GABA_A$ receptor heterogeneity between the hypothalamus and cortex. J Chem Neuroanat. 7:243–252.
Jacob TC, Bogdanov YD, Magnus C, Saliba RS, Kittler JT, Haydon PG, Moss SJ. 2005. Gephyrin regulates the cell surface dynamics of synaptic $GABA_A$ receptors. J Neurosci. 25:10469–10478.
Jiao Y, Zhang C, Yanagawa Y, Sun QQ. 2006. Major effects of sensory experiences on the neocortical inhibitory circuits. J Neurosci. 26:8691–8701.
Kang TC, An SJ, Park SK, Hwang IK, Bae JC, Won MH. 2003. Changed vesicular GABA transporter immunoreactivity in the gerbil hippocampus following spontaneous seizure and vigabatrin administration. Neurosci Lett. 335:201–211.
Kilman V, van Rossum MCW, Turrigiano GG. 2002. Activity deprivation reduces miniature IPSC amplitude by decreasing the number of postsynaptic $GABA_A$ receptors clustered at neocortical synapses. J Neurosci. 22:1328–1337.
Kitzes LM. 1984. Some physiological consequences of neonatal cochlear destruction in the inferior colliculus of the gerbil, Meriones unguiculatus. Brain Res. 306:171–178.
Kitzes LM, Semple MN. 1985. Single-Unit Responses in the Inferior colliculus: effects of neonatal unilateral cochlear ablation. J Neurophys. 53:1483–1500.
Korada S, Schwartz IR. 1999. Development of GABA, glycine and their receptors in the auditory brainstem of gerbil: a light and electron microscopic study. J Comp Neurol. 409:664–681.
Kotak VC, Fujusawa S, Lee FA, Karthikeyan O, Aoki C, Sanes DH. 2005. Hearing loss raises excitability in the auditory cortex. J Neurosci. 25:3908–3918.

Kotak VC, Sanes DHS. 1996. Developmental influence of glycinergic transmission: regulation of NMDA receptor-mediated EPSPs. J Neurosci. 16:1836–1843.
Kotak VC, Takesian AE, Sanes DH. Forthcoming. Hearing loss prevents the maturation of GABAergic transmission in the auditory cortex. Cerebral Cortex.
MacDonald RL, Olsen RW. 1994. GABAA receptor channels. Annu Rev Neurosci. 17:569–602.
Maffei A, Nelson SB, Turrigiano GG. 2004. Selective reconfiguration of layer 4 visual cortical circuitry by visual deprivation. Nat Neurosci. 7:1353–1359.
McAlpine D, Martin RL, Mossop JE, Moore DR. 1997. Response properties of neurons in the inferior colliculus of the monaurally deafened ferret to acoustic stimulation of the intact ear. J Neurophysiol. 78:767–779.
Maqueda J, Ramirez M, Lamas M, Gutierrez R. 2003. Glutamic acid decarboxylase (GAD)67, but not GAD65, is constitutively expressed during development and transiently overexpressed by activity in the granule cells of the rat. Neurosci Lett. 353:69–71.
Martin DL, Rimvall R. 1993. Regulation of γ-aminobutyric acid synthesis in the brain. J Neurochem. 60:395–407.
Maxwell DJ, Christie WM, Short AD, Brown AG. 1990. Direct observations of synapses between GABA-immunocreactive boutons and muscle afferent terminals in lamina VI of the cat's spinal cord. Brain Res. 530:215–222.
Meier J, Grantyn R. 2004. A gephyrin-related mechanism restraining glycine receptor anchoring at GABAergic synapses. J Neurosci. 24:1398–1405.
Micheva KD, Beaulieu C. 1995. Neonatal sensory deprivation induces selective changes in the quantitative distribution of GABA-immunoreactive neurons in the rat barrel field cortex. J Comp Neurol. 361:574–584.
McKernan RM, Whiting PJ. 1996. Which $GABA_A$-receptor subtypes really occur in the brain? Trends Neurosci. 19:139–143.
Milbrandt JC, Holder TM, Wilson MC, Salvi RJ, Caspary DM. 2000. GAD levels and muscimol binding in rat inferior colliculus following acoustic trauma. Hear Res. 147:251–260.
Möhler H. 2006. GABAA receptor diversity and pharmacology. Cell Tissue Res. 326:505–516.
Mouton PR. 2002. Principles and Practices of Unbiased Stereology: An Introduction for Bioscientists. Baltimore, MD: Johns Hopkins University Press. p. 1–236.
Mower GD, Rustad R, White WF. 1988. Quantitative comparisons of gamma-aminobutyric acid neurons and receptors in the visual cortex of normal and dark-reared cats. J Comp Neurol. 272:293–302.
Mower GD, White WF, Rustad R. 1986. [3H]muscimol binding of GABA receptors in the visual cortex of normal and monocularly. Brain Res. 380:253–260.
Mossop JR, Wilson MJ, Caspary DM, Moore DR. 2000. Down-regulation of inhibition following unilateral deafening. Hear Res. 147:183–187.
Mower GD, Guo Y. 2001. Comparison of the expression of two forms of glutamic acid decarboxylase (GAD67 and GAD65) in the visual cortex of normal and dark-reared cats. Dev Brain Res. 126:65–74.
Mugnaini E, Oertel WH. 1985. An atlas of the distribution of GABAergic neurons and terminals in the rat CNS as revealed by GAD immunohistochemistry. In: Björklund A, Hökfelt T, editors. GABA and neuropeptides in the CNS. Vol. 4. New York: Elsevier. p. 436–595.
Muzio L, DiBenedetto B, Stoykova A, Boncinelli E, Gruss P, Mallamaci A. 2002. Conversion of cerebral cortex into basal ganglia in Emx2(-/-) Pax6(Sey/Sey) double mutant mice. Nat Neurosci. 5:737–745.
Nusser Z, Cull-Candy S, Farrant M. 1997. Differences in synaptic $GABA_A$ receptor number underlie variation in GABA mini amplitude. Neuron. 19:697–709.
Nusser Z, Hajos N, Somogyi P, Mody I. 1998. Increased number of synaptic $GABA_A$ receptors underlies potentiation at hippocampal inhibitory synapses. Nature. 395:172–177.
Orozco-Suarez S, Brunson KL, Feria-Velasco A, Ribak CE. 2000. Increased expression of gamma-aminobutyric acid transporter-1 in the forebrain of infant rats with corticotropin-releasing hormone-induced seizures but not in those with hyperthermia-induced seizures. Epilepsy Res. 42:141–157.
Peters A, Saint Marie RL. 1984. Smooth and sparsely spinous non-pyramidal cells forming local axonal plexuses. In: Peters A, Jones EG, editors. Cerebral cortex, cellular components of the cerebral cortex. Vol. 1. New York: Plenum Press. p. 419–446.
Petersen SA, Fetter RD, Noordermeer JN, Goodman CS, DiAntonio A. 1997. Genetic analysis of glutamate receptors in drosophila reveals a retrograde signal regulating presynaptic transmitter release. Neuron. 19:1237–1248.
Rajan R. 1998. Receptor organ damage causes loss of cortical surround inhibition without topographic map plasticity. Nat Neurosci. 1:138–143.
Ramirez M, Gutierrez R. 2001. Activity-dependent expression of GAD67 in the granule cells of the rat hippocampus. Brain Res. 917:139–46.
Richards JG, Schoch P, Häring P, Takács B, Möhler H. 1987. Resolving GABAA/benzodiazepine receptors: cellular and subcellular localization in the CNS with monoclonal antibodies. J Neurosci. 7:1866–1886.
Rimvall K, Martin DL. 1994. The level of GAD67 protein is highly sensitive to small increases in intraneuronal gamma-aminobutyric acid levels. J Neurochem. 62:1375–1381.
Rutledge LT. 1978. The effects of denervation and stimulation upon synaptic ultrastructure. J Comp Neurol. 178:117–128.
Salvi RJ, Wange J, Ding D. 2000. Auditory plasticity and hyperactivity following cochlear damage. Hear Res. 147:261–274.
Sanes DH, Markowitz S, Bernstein J, Wardlow J. 1992. The influence of inhibitory afferents on the development of postsynaptic dendritic arbors. J Comp Neurol. 321:637–644.
Shepherd GM, Pologruto TA, Svoboda K. 2003. Circuit analysis of experience-dependent plasticity in the developing rat barrel cortex. Neuron. 2003(38):277–289.
Silver MA, Stryker MP. 2000. Distributions of synaptic vesicle proteins and GAD65 in deprived and nondeprived ocular dominance columns in Layer IV of kitten primary visual cortex are unaffected by monocular deprivation. J Comp Neurol. 422:652–664.
Studler B, Sidler C, Fritschy JM. 2005. Differential regulation of GABAA receptor and gephyrin postsynaptic clustering in immature hippocampal neuronal cultures. J Comp Neurol. 484:344–355.
Tehrani MH, Barnes EM, Jr. 1991. Agonist-dependent internalization of gamma-aminobutyric acid A/benzodiazepine receptors in chick cortical neurons. J Neurochem. 57:1307–1312.
Tierney TS, Moore DR. 1997. Naturally occurring neuron death during postnatal development of the gerbil ventral cochlear nucleus begins at the onset of hearing. J Comp Neurol. 387:421–429.
Tongjaroenbungam W, Jongkamonwiwat N, Cunningham J, Phansuwan-Pujito P, Dodson HC, Forge A, Govitrapong P, Casalotti SO. 2004. Opioid modulation of GABA release in the rat inferior colliculus. BMC Neurosci. 5:31.
Trachtenberg JT, Stryker MP. 2001. Rapid anatomical plasticity of horizontal connections in the developing visual cortex. J Neurosci. 21:3476–3482.
Turecek R, Trussell LO. 2002. Presynaptic glycine receptors enhance transmitter release at a mammalian central synapse. Nature. 411:587–590.
Turrigiano G. 2007. Homeostatic signaling: the positive side of negative feedback. Curr Opin Neurobiol. 17:318–324.
Vale C, Sanes DH. 2002. The effect of bilateral deafness on excitatory and inhibitory synaptic strength in the inferior colliculus. Eur J Neurosci. 16:2394–2404.
Vale C, Schoorlemmer J, Sanes DH. 2003. Deafness disrupts chloride transporter function and inhibitory synaptic transmission. J Neurosci. 23:7516–7524.
Vale C, Juiz JM, Moore DR, Sanes DH. 2004. Unilateral cochlear ablation produces greater loss of inhibition in the contralateral inferior colliculus. Eur J Neurosci. 20:2133–2140.
Verdoorn TA, Draguhn A, Ymer S, Seeburg PH, Sakmann B. 1990. Functional properties of recombinant rat $GABA_A$ receptors depend on subunit composition. Neuron. 4:919–928.
Wafford KA, Bain CJ, Quirk K, McKernan RM, Wingrove PB, Whiting PJ, Kemp JA. 1994. A novel allosteric modulatory site on the GABAA receptor beta subunit. Neuron. 12:775–782.
Wierenga CJ, Walsh MF, Turrigiano GG. 2006. Temporal regulation of the expression locus of homeostatic plasticity. J Neurophysiol. 96:2127–2133.
Wisden W, Laurie DJ, Monyer H, Seeburg PH. 1992. The distribution of 13 GABA, receptor subunit mRNAs in the rat brain. I. Telencephalon, diencephalon, mesencephalon. J Neurosci. 12: 1040–1062.